Heliyon 9 (2023) e20012

Contents lists available at ScienceDirect

Heliyon

journal homepage: www.cell.com/heliyon

Shiga toxin 2 A-subunit induces mitochondrial damage, mitophagy and apoptosis via the interaction of Tom20 in Caco-2 cells

Jie Tang [a,1], Xiaoxue Lu [b,1], Tao Zhang [a], Yuyang Feng [b], Qiaolin Xu [a], Jing Li [a], Yuanzhi Lan [a], Huaxing Luo [a], Linghai Zeng [a], Yuanyuan Xiang [a], Yan Zhang [a], Qian Li [b], Xuhu Mao [b], Bin Tang [c,**], Dongzhu Zeng [a,*,2]

[a] Department of General Surgery, The Third Affiliated Hospital of Chongqing Medical University, Chongqing, 401120, China
[b] Department of Clinical Microbiology and Immunology, College of Pharmacy and Medical Laboratory, Army Medical University (Third Military Medical University), Chongqing, 400038, China
[c] Department of Clinical Laboratory, Chongqing University Jiangjin Hospital, School of Medicine, Chongqing University, Jiangjin, Chongqing, 402260, China

ARTICLE INFO

Keywords:
Shiga toxin
Shiga toxin type 2
Mitophagy
Apoptosis
Tom20

ABSTRACT

Shiga toxin type 2 (Stx2) is the primary virulence factor produced by Shiga toxin-producing enterohemorrhagic *Escherichia coli* (STEC), which causes epidemic outbreaks of gastrointestinal sickness and potentially fatal sequela hemolytic uremic syndrome (HUS). Most studies on Stx2-induced apoptosis have been performed with holotoxins, but the mechanism of how the A and B subunits of Stx2 cause apoptosis in cells is not clear. Here, we found that Stx2 A-subunit (Stx2A) induced mitochondrial damage, PINK1/Parkin-dependent mitophagy and apoptosis in Caco-2 cells. PINK1/Parkin-dependent mitophagy caused by Stx2A reduced apoptosis by decreasing the accumulation of reactive oxidative species (ROS). Mechanistically, Stx2A interacts with Tom20 on mitochondria to initiate the translocation of Bax to mitochondria, leading to mitochondrial damage and apoptosis. Overall, these data suggested that Stx2A induces mitochondrial damage, mitophagy and apoptosis via the interaction of Tom20 in Caco-2 cells and that mitophagy caused by Stx2A ameliorates apoptosis by eliminating damaged mitochondria. These findings provide evidence for the potential use of Tom20 inhibition as an anti-Shiga toxin therapy.

1. Introduction

Shiga toxins (Stxs), which are major virulence factors produced by Shiga toxin-producing enterohemorrhagic *Escherichia coli* (STEC), can cause hemorrhagic colitis (HC), hemolytic uremic syndrome (HUS), microangiopathic hemolytic anemia and renal failure [1]. All members of the Stxs are a group of bacterial AB5 protein toxins [2]. The A-subunit is an N-glycosidase that removes an adenine

* Corresponding author.
** Corresponding author.
E-mail addresses: tangbin118@cqu.edu.cn (B. Tang), zdz@hospital.cqmu.edu.cn (D. Zeng).
[1] Jie Tang and Xiaoxue Lu contributed equally to this work.
[2] Lead contact.

https://doi.org/10.1016/j.heliyon.2023.e20012
Received 23 March 2023; Received in revised form 18 August 2023; Accepted 8 September 2023
Available online 9 September 2023

residue from the 28S rRNA of the 60S ribosome, making the ribosome inactive for protein synthesis [3,4]. The B-subunit (Stx B) binds to the globotriaosylceramide (Gb3) glycolipid of the eukaryotic cell membrane [5]. After binding, Stxs travel from the endosome to the Golgi and then to the endoplasmic reticulum [6]. In recent years, numerous studies have found that Shiga toxins induce apoptosis of intestinal epithelial cells by activating various signaling pathways, such as the ribosomal toxic stress response and endoplasmic reticulum stress [7,8]. These previous studies on Stx-induced apoptosis were performed with holotoxins, but the mechanism of how the A and B subunits of Stx2 cause apoptosis in cells is not clear.

As the energy generators of cells, mitochondria have emerged as key players in maintaining cellular homeostasis [9]. Dysfunctional mitochondria lead to the destruction of intracellular homeostasis and even induce cell death [10]. Previous studies have reported several serotypes of STEC that induce apoptosis in various cells, such as monocytic, neuronal, lymphoid and epithelial cells [8,11–13]. It has been reported that apoptosis induced by Stxs is accompanied by damaged mitochondria, cytochrome *c* release and mitochondrial membrane potential reduction in epithelial cells [14]. These results indicate that Stxs may induce apoptosis through the mitochondrial pathway in epithelial cells.

Mitophagy, which is a main mitochondrial quality control mechanism for eliminating damaged mitochondria, participates in the regulation of cellular bioenergetics, metabolism, proliferation and death [15]. Mitophagy is an essential process that helps maintain mitochondria in good working order under physiological circumstances by removing unhealthy or unnecessary mitochondria [16]. However, persistent and/or severe mitophagy may result in mitochondrial malfunction and even cell death. Previous studies have reported that Shiga toxins induce autophagy through the endoplasmic reticulum (ER) stress pathway in human intestinal or renal epithelial cells [17,18]. Although Shiga toxins induce mitochondrial damage and autophagy, it is unclear whether the mitochondria damaged by Shiga toxins can be eliminated by mitophagy in intestinal epithelial cells.

In the present study, we demonstrated that Stx2 or the Stx2 A-subunit (Stx2A) promoted apoptosis, mitochondrial damage and PINK1/Parkin-dependent mitophagy in Caco-2 cells. In addition, Stx2A may recruit Bax translocation to mitochondria in association with Tom20 on the mitochondrial outer membrane, causing mitochondrial damage, mitophagy and apoptosis in Caco-2 cells. Overall, these findings will contribute to a more comprehensive understanding of the mechanisms by which Stx2A-induced mitophagy inhibits intestinal epithelial apoptosis.

2. Materials and methods

2.1. Antibodies, reagents, siRNA and shRNA

The following antibodies were utilized in the present study: MnSOD (ab137037), cytochrome *c* (ab13575) and Parkin (ab77924, ab15494) from Abcam (Shanghai, China); SQSTM1 (88588), LC3B (83506), COX IV (4850), Cleaved-Caspase-3 (9661), PINK1 (6946), Tom20 (42406), Cleaved-Caspase-9 (20750), Bax (2772), GAPDH (2118), Beclin-1 (3738) and Hsp60 (12165) from Cell Signaling Technology (Shanghai, China); Bcl-2 (12789), Bax (60267) and VDAC1 (66345) from Proteintech (Wuhan, China); and PINK1 (BC100–494) and 8-OHdG (NB110-96878) from Novas Biologicals (Shanghai, China). MitoTracker Red CMXRos (C1035), FITC-labeled goat anti-mouse IgG (A0568) and DAPI (C1002) were purchased from Beyotime (Shanghai, China). All horseradish peroxidase-conjugated secondary antibodies (7076P2 and 7074S) were purchased from Cell Signaling Technology (Shanghai, China). Fluorescence secondary antibodies (Alexa Fluor® 488, ab150073; Alexa Fluor® 555, ab150074) were obtained from Abcam. MitoSOX (M36008) was obtained from Invitrogen, and bafilomycin A1, lactacystin and MitoTEMPO (SML0737) was obtained from Sigma (Shanghai, China). SiRNA and shRNA were synthesized by the Allwegene Technology Co., Ltd. (Beijing, China). The following shRNA and siRNA sequences were derived from other studies: PINK1 siRNA [19], 5′-GAGUAGCCGCAAAUGUGCUUCU-3’; Parkin siRNA [19], 5′-UCCAGCUCAAGGAGGUGGUGCUAA-3’; Tom20 shRNA [20], 5′-GCTAGCTGTGTCGAGTTAA-3′ [2]; and BAX shRNA [20], 5′-GCTGGACATTGGACTTCCT-3′ [2].

2.2. Cell culture

The Caco-2 human intestinal epithelial cell line was obtained from the Cell Bank at the Chinese Academy of Sciences. Caco-2 cells were cultured in DMEM (11965–092, Gibco) containing 10% fetal bovine serum (FBS) (10099–141, Gibco) and 100 U/ml penicillin/streptomycin (15140–122, Gibco) at 37 °C in an incubator with 5% CO_2.

2.3. Construction of the Stx2A and Stx2B plasmids

The Stx2A and Stx2B plasmids were synthesized by Allwegene Technology Co., Ltd. (Beijing, China). To construct recombinant expression plasmids, the Stx2A and Stx2B sequences were amplified using primers, and the gene sequences were cloned into the *Hin*dIII-*Eco*RI sites in the pcDNA3.1 and pEGFP-N1 vectors with Flag tags added to the C-terminal and N-terminal, respectively. Human codon optimization was performed, and an empty vector was used as a control. The primer sequences are listed in Supplementary Table 1 and Table 2.

2.4. Cell viability assay

A Cell Counting Kit-8 (CCK-8 Kit) (CK04, Dojindo) was used to analyze cell viability according to the manufacturer’s instructions. Briefly, Caco-2 cells per (1000 cells/100 μL) in 96-well plates were transfected with Stx2A, Stx2B or Stx2A/2B plasmids (1 μg/ml) for 0,

12, 24 and 48 h. Then, 10 μL of CCK-8 reagent was added to 96-well plates (1×10^3 cells/well) followed by incubation at 37 °C for 1 h. The absorbance at 450 nm was measured using a microplate reader (iMark; Bio-Rad).

2.5. Cell ultrastructure analysis

The Stx2A-transfected Caco-2 cell samples were placed into 1.5-mL EP tubes and centrifuged at 100×*g* for 10 min. Caco-2 cells were then fixed in a solution containing 3% glutaraldehyde and 0.1 M sodium cacodylate at 4 °C overnight followed by postfixation with 1% osmium tetroxide (OsO_4) at 25 °C for 2 h. The cell samples were then dehydrated in an acetone gradient, embedded in Epon 812 and cut into ultrathin sections. After staining the sections with 2% uranyl acetate and 0.3% lead citrate, they were examined using a JEM-1400PLUS transmission electron microscope (Japan).

2.6. Analysis of mitochondrial ROS

MitoSOX (M36008, Invitrogen), a mitochondrial-specific indicator, was used to detect the mitochondrial ROS levels in Caco-2 cells. After Stx2A and/or Mito-TEMPO treatments, Caco-2 cells were stained with MitoSOX (5 μM) or Hoechst (C1017, Beyotime) for 30 min at 37 °C followed by three washes with PBS to remove excess dye. The fluorescence of MitoSOX Red was detected by an Amnis® FlowSight® Imaging Flow Cytometer and analyzed by Amnis IDEAS software v6.2 or detected by confocal microscopy (Leica STELLARIS STED) for imaging.

2.7. Analysis of mitochondrial membrane potential

After Stx2A and/or Mito-TEMPO treatments, Caco-2 cells were stained with JC-1 (500 μl) using a JC-1 staining kit (C2006, Beyotime) for 20 min at 37 °C and washed twice with 1 ml of JC-1 staining buffer. The fluorescence was detected by an Amnis® FlowSight® Imaging Flow Cytometer. The ratio of red-to-green fluorescence intensity was used to determine the MMP. The fluorescence of green (Ex/Em = 514/529 nm) and red (Ex/Em = 585/590 nm) was analyzed by Amnis IDEAS software v6.2.

2.8. Analysis of apoptosis

Apoptotic cells were detected with an Annexin V-FITC/PI Apoptosis Detection Kit (C1062, Beyotime) according to the manufacturer's instructions. The cells were first trypsinized with 0.25% trypsin for 3 min, centrifuged at 1000×*g* for 5 min and gently resuspended in 195 μl of Annexin V-FITC binding solution combined with 10 μl of propidium iodide staining solution and 5 μl of annexin V-FITC. After incubation for 15 min at room temperature (20–25 °C) in the dark, the samples were placed in an ice bath and then detected by an Amnis® FlowSight® Imaging Flow Cytometer. Amnis IDEAS software v6.2 was used to evaluate the fluorescence.

2.9. Quantification of mtDNA

DNA was extracted using a MiniBEST Universal Genomic DNA Extraction kit (9765, Takara) according to the manufacturer's instructions. A NanoDrop One Microvolume UV–Vis Spectrophotometer (Thermo Scientific, USA) was used to assess the quantity of DNA in the extracts, and real-time PCR was used to determine the number of copies of mtDNA. Mitochondrial cytochrome *c* oxidase subunit 1 (mtCO1) was used as a mitochondrial DNA marker, while ribosomal protein L13a (RPL13A) was used as a nuclear DNA marker. The primer sequences of mtCO1 and RPL13A are as following: mtCO1 (forward, 5′-CAGGAGTAGGAGAGAGGGAGGTAAG-3'; reverse, 5′-TACCCATCATAATCGGAGGCTTTGG-3′) as mitochondrial DNA markers, RPL13A (forward, 5′-CGCCCTACGACAAGAAAAAG-3'; reverse, 5′-CCGTAGCCTCATGAGCTGTT-3′) was also detected as a marker of nuclear DNA. The relative amounts of mitochondrial DNA and nuclear DNA copy numbers were calculated.

2.10. Immunofluorescence staining

For staining, Caco-2 cells were grown on cell slides. Living Caco-2 cells were treated with MitoTracker Red (100 nM) for 30 min at 37 °C to label mitochondria and subsequently fixed with 4% PFA. Cells were then permeabilized with 0.1% Triton-X-100 for 5 min at room temperature followed by incubation with LC3B, PINK1, Parkin, 8-OHdG, Tom20, Hsp60 and Bax antibodies (1:100) overnight at 4 °C. Following secondary antibody incubation, images were acquired using a confocal microscope (Leica STELLARIS STED) at a wavelength appropriate for MitoTracker Red (550 nm) and fluorescent secondary antibodies (corresponding wavelength).

2.11. Coimmunoprecipitation assay

Caco-2 cells transfected with Stx2A-Flag plasmids or control pcDNA3.1 plasmids were lysed using lysis buffer containing 50 mM Tris (pH 7.5), 2.5 mM sodium pyrophosphate, 1% Triton X-100, 1 mM EDTA, 1 mM EGTA, 150 mM NaCl and 1 mM PMSF. The proteins were immunoprecipitated with anti-Flag magnetic beads (M8823, Sigma−Aldrich, Shanghai). Western blot was used to examine the input and immunoprecipitation samples using Flag and Tom20 antibodies.

2.12. Western blot analysis

Caco-2 cells were lysed with cold RIPA buffer (P0013B, Beyotime) containing protease and phosphatase inhibitors followed by centrifugation at 4 °C for 20 min at 5000 g. The protein concentration was measured with a BCA protein assay kit (Pierce, 23227). The lysates were separated using SDS–PAGE and then transferred to PVDF membranes (A10600023, GE Healthcare Life Science). The membranes were first incubated with various primary antibodies overnight at 4 °C and then incubated with secondary antibodies for an additional hour at 25 °C. The protein bands were detected by the ChemiDoc Touch Imaging System (Bio-Rad).

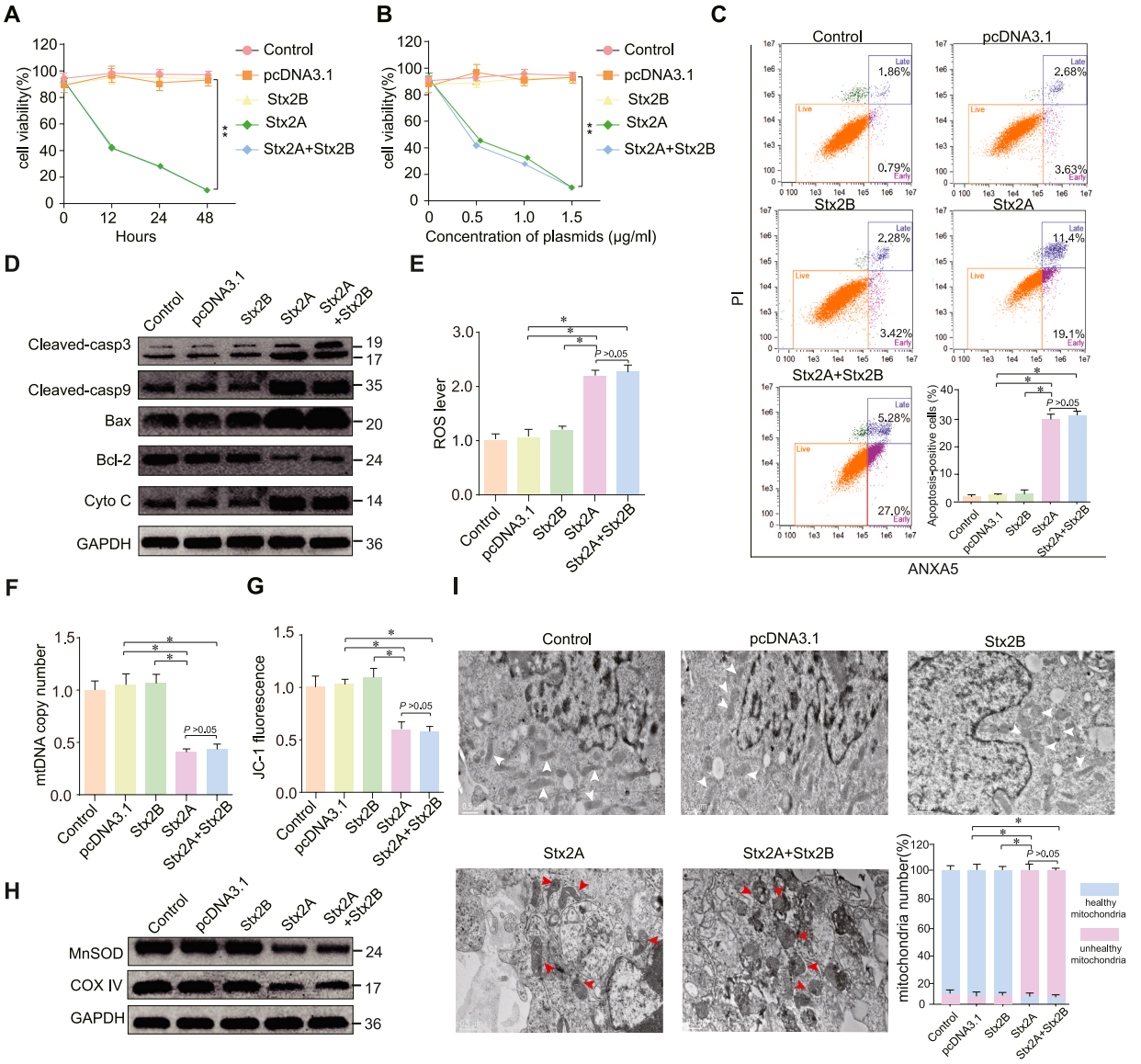

Fig. 1. Stx2A induces apoptosis and mitochondrial damage in Caco-2 cells. (A, B) The effects of Stx2 submits on cell viability were analyzed with a CCK-8 assay. In the time-course experiments (A), Caco-2 cells were transfected with 1 μg/ml pcDNA3.1, Stx2B, Stx2A and Stx2A/2B plasmids for 12, 24 and 48 h. In the dose-dependent experiments (B), Caco-2 cells were transfected with 0, 0.5, 1 or 1.5 μg/ml plasmids of expressing Stx2A/2B for 24 h. (C–I) After transfected with 1 μg/ml pcDNA3.1, Stx2B, Stx2A or Stx2A/2B plasmids for 24 h, Caco-2 cells were subjected to ANXA5-PI staining and analyzed by flow cytometry (C), and Western blot analysis (D) of Cleaved-Caspase-3, Cleaved-Caspase-9, Bax, cytochrome *c* (Cyto C) and Bcl-2, and quantification of mitochondrial superoxide levels (E) and MMP by flow cytometry (G), and quantification of mtDNA copy number by qPCR analysis (F), and the protein expression levels of MnSOD and COX IV were evaluated by Western blot analysis (H), and mitochondrial ultrastructure was evaluated by TEM (I). The red arrows represent the damaged mitochondrias, and the white arrows represent the healthy mitochondrias. n = 3. $^{*}P < 0.05$, $^{**}P < 0.01$.

2.13. FLAG pull-down

Caco-2 cells with or without Stx2A-Flag expression were lysed and immunoprecipitated using magnetic anti-Flag beads (M8823, Sigma–Aldrich, Shanghai). The distinctive bands of the Stx2A-Flag pulled-down sample were excised for subsequent in-gel trypsin digestion after the purified protein complexes were separated by SDS–PAGE and stained with Coomassie brilliant blue. A nano-ACQUITY UPLC system (Waters Corporation, Boston, USA) coupled to a Q-Exactive HF-X was used for the LC–MS/MS analysis (ThermoFisher Scientific). The data analysis from LC-MS/MS files were processed using Proteome Discoverer (PD) software (Version 2.4.0.305) and the built-in Sequest HT search engine. MS spectra lists were searched against their species-level UniProt FASTA databases (uniprot-Homo sapiens-9606-2021-8. fasta), Carbamidomethyl as a fixed modification, Oxidation and Acetyl (Protein N-term) as variable modifications. Trypsin was used as proteases. A maximum of 2 missed cleavage(s) was allowed. The false discovery rate (FDR) was set to 0.01 for both PSM and peptide levels. Peptide identification was performed with an initial precursor mass deviation of up to 10 ppm and a fragment mass deviation of 0.02 Da. The data of the LC–MS/MS analysis has been deposited to the ProteomeXchange Consortium (http://proteomecentral.proteomexchange.org) via the iProX partner repository with the dataset identifier PXD038256.

2.14. GO and KEGG pathway enrichment analyses

The proteins discovered by LC–MS/MS were submitted to DAVID Bioinformatics Resources 6.8 for GO enrichment analysis and KEGG pathway analysis using the ggplot2 package in R (version 4.0.3, R Core Team; R Foundation for Statistical Computing, Vienna, Austria) (Supplementary Table 3).

2.15. Docking of Stx2A and Tom20

M-ZDOCK was used to dock the modules of Stx2A and Tom20. The three-dimensional (3D) models of Stx2A and Tom20 proteins were generated using the Phyre2 server (http://www.sbg. bio. ic.ac.uk/phyre2), and Stx2A and Tom20 were then imported into ZDOCK to simulate possible combinations using Biovia Discovery Studio Client 2019 (BIOVIA Corp., San Diego, CA, USA).

2.16. Statistical analysis

Data were analyzed using IBM SPSS Statistics 20.0 software (IBM Inc., Armonk, NY, USA) and GraphPad Prism 6 software (GraphPad Inc., San Diego, CA, USA). Student's *t*-test was utilized to compare data between two groups. One-way analysis of variance (ANOVA) was used to compare data from different groups. Differences with $^{*}P < 0.05$ or $^{**}P < 0.01$ were considered statistically significant.

3. Results

3.1. Stx2A induces apoptosis and mitochondrial damage in Caco-2 cells

Previous studies have shown that Shiga toxin 2 (Stx2) causes rapid apoptosis and autophagic cell death via the ER stress pathway in human retinal or intestinal epithelial cells [21]. However, it is not clear which subunit of Stx2 plays a toxic role. To further study the toxicity of Stx2 subunits in intestinal epithelial cells, Caco-2 cells were transfected with Stx2A, Stx2B, or Stx2A/2B eukaryotic expression plasmids, and the viability of Caco-2 cells was examined in time-course experiments. As shown in Fig. 1A, the cell viability of the Stx2A and Stx2A/2B groups was significantly decreased compared to that of the control, pcDNA3.1 and Stx2B groups, and there was a gradual decrease over time in the Stx2A and Stx2A/2B groups. Similar results were also obtained in Stx2A or Stx2A/2B dose-dependent experiments in Caco-2 cells (Fig. 1B). Moreover, an Annexin V-FITC/propidium iodide (PI) staining assay showed that Stx2A or Stx2A/2B significantly increased cell death in Caco-2 cells (Fig. 1C). In addition, apoptosis-related proteins were detected by Western blot analysis in Stx2A, Stx2B, or Stx2A/2B transfected Caco-2 cells. Stx2A or Stx2A/2B significantly increased the expression of Cleaved-Caspase-3 (Cleaved-Casp3), Cleaved-Caspase-9 (Cleaved-Casp9), Bax and cytochrome *c* (Cyto C) but decreased the expression of Bcl-2 (Fig. 1D). These results indicated that Stx2A, but not Stx2B, induces apoptosis.

Previous studies have shown that Shiga toxins trigger mitochondrial damage, leading to apoptosis in HeLa cells or human retinal epithelial cells [14,21]. To elucidate whether Stx2A induces mitochondrial damage in Caco-2 cells, we applied flow cytometry or quantitative real-time PCR to detect mitochondrial superoxide levels, mitochondrial membrane potential (MMP) and mtDNA copy number after transfection with the Stx2 plasmids. Stx2A significantly elevated the mitochondrial ROS levels (Fig. 1E) but reduced the mtDNA copy number and MMP in Caco-2 cells (Fig. 1F and G). In addition, Stx2A or Stx2A/2B markedly decreased the expression of manganese superoxide dismutase (MnSOD) and cytochrome *c* oxidase subunit IV (COX IV) protein levels in Caco-2 cells (Fig. 1H). Moreover, prominent structural damage to mitochondria was observed by transmission electron microscopy (TEM) after transfection of Stx2A or Stx2A/2B (Fig. 1I). These data suggested that Stx2A induces apoptosis and mitochondrial damage in Caco-2 cells.

3.2. Stx2A induces mitophagy in Caco-2 cells

Mitophagy is important for mitochondrial quality control. In the early stage of mitophagy, the mitophagosome can be identified by

its unique bilayer membrane and cristae, and in the late stage, the mitolysosome formed by fusion of the mitophagosome with the lysosome can be generally recognised by its monolayer structure or digested residue [22,23]. After transfection with Stx2A plasmids, we evaluated several markers of mitophagy in Caco-2 cells. TEM assays showed that numerous mitochondria were engulfed in autophagosomes and degraded in autolysosomes at 24 h or 48 h following Stx2A transfection (Fig. 2A). Consistent with the TEM findings, the expression levels of LC3BII and Beclin1 (autophagy biomarkers) were increased, while SQSTM1 and the mitochondrial outer membranous protein, Tom20, were decreased by Stx2A compared to cells in the control group in a time-dependent manner (Fig. 2B). Further immunofluorescence staining of LC3B and MitoTracker Red, a red-fluorescent dye that stains mitochondria in live cells, revealed increased mitophagy in a time-dependent manner in Caco-2 cells transfected with Stx2A (Fig. 2C). These data demonstrated that Stx2A induces mitophagy in Caco-2 cells.

3.3. PINK1 and parkin mediate Stx2A-induced mitophagy

Because Stx2A induced mitochondrial injury and mitophagy, we next investigated whether Stx2A-induced mitophagy depends on the PINK1/Parkin pathway. Subsequently, the expression of PINK1/Parkin proteins was evaluated by Western blot in Caco-2 cells transfected with Stx2A. As shown in Fig. 3A, Stx2A significantly increased the protein expression of PINK1 and Parkin after transfection with Stx2A plasmids for 24 h. In addition, PINK1 and Parkin protein levels in mitochondria were also significantly increased (Fig. 3B). In response to Stx2A, the protein expression levels of PINK1 and Parkin were increased in Caco-2 cells, and their colocalization with MitoTracker was increased in a time-dependent manner (Fig. 3C–D). To elucidate the PINK1-Parkin pathway of mitophagy in Caco-2 cells transfected with Stx2A, PINK1 or Parkin was knocked down by siRNA. Immunofluorescence showed that knockdown of PINK1 or Parkin decreased Stx2A-induced PINK1/Parkin-mediated mitophagy as assessed by costaining of Parkin and LC3B (Fig. 3E). Moreover, knockdown of PINK1 or Parkin decreased the expression of LC3BII but increased the expression of SQSTM1 and Tom 20 (Fig. 3F). These data indicated that PINK1 and Parkin mediate Stx2A-induced mitophagy in Caco-2 cells.

3.4. PINK1/parkin-dependent mitophagy decreases mitochondrial ROS production and apoptosis induced by Stx2A

To clarify the regulatory effect of PINK1/Parkin-dependent mitophagy on mitochondrial ROS production, we used MitoSOX or 8-OHdG to label mitochondrial superoxide or DNA oxidative damage in Caco-2 cells transfected with Stx2A. As shown in Fig. 4A, Stx2A increased mitochondrial ROS and DNA oxidative damage, and a more significant increase was observed after PINK1 or Parkin was knocked down. Moreover, knockdown of PINK1 or Parkin significantly increased the mitochondrial ROS levels induced by Stx2A (Fig. 4B). Mito-TEMPO is a mitochondrial target superoxide dismutase mimic that scavenges superoxide and alkyl free radicals. As shown in ,Fig. 4A–B Mito-TEMPO reduced mitochondrial ROS and DNA oxidative damage in Stx2A-transfected Caco-2 cells after silencing PINK1 or Parkin. Compared to Stx2A-transfected cells, the protein expression of LC3BII, PINK1, Parkin and Beclin1 was

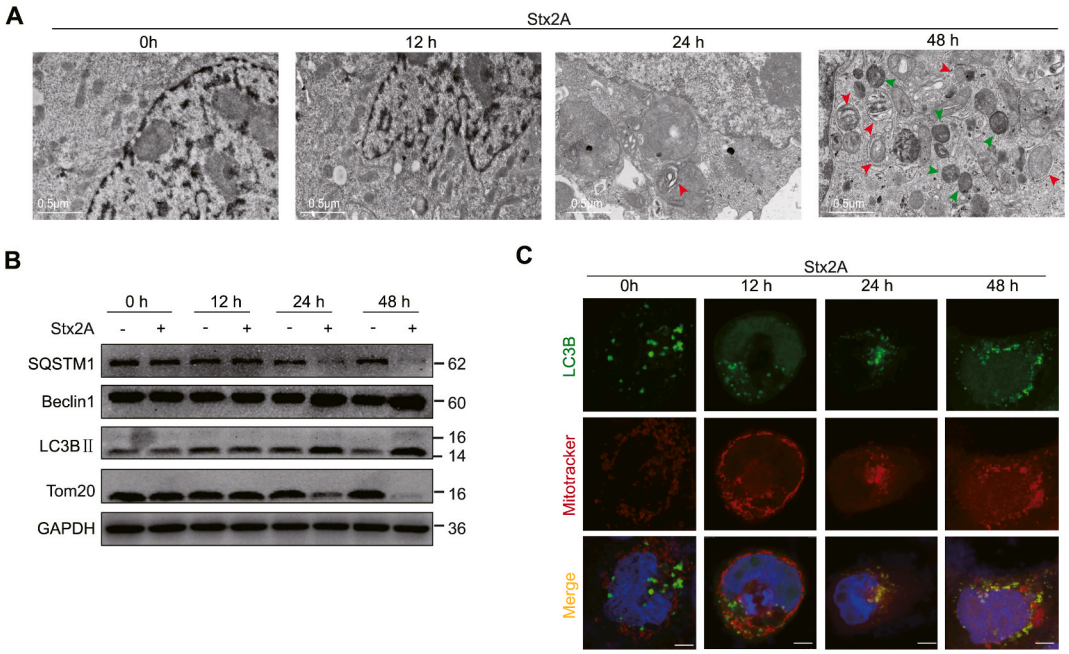

Fig. 2. Stx2A induces mitophagy in Caco-2 cells. (A–C) Caco-2 cells were transfected with 1 μg/ml Stx2A plasmids for 12, 24 and 48 h. TEM images (A) of Caco-2 cells showing mitophagosomes (red arrow) and mitolysosomes (green arrow). The protein expression of LC3 II/I, Beclin1, Tom20 and SQSTM1 was detected by Western blot analysis (B). Colocalization of MitoTracker Red (Red), LC3B (Green) and DAPI (Blue) (C). Scale bar = 5 μm.

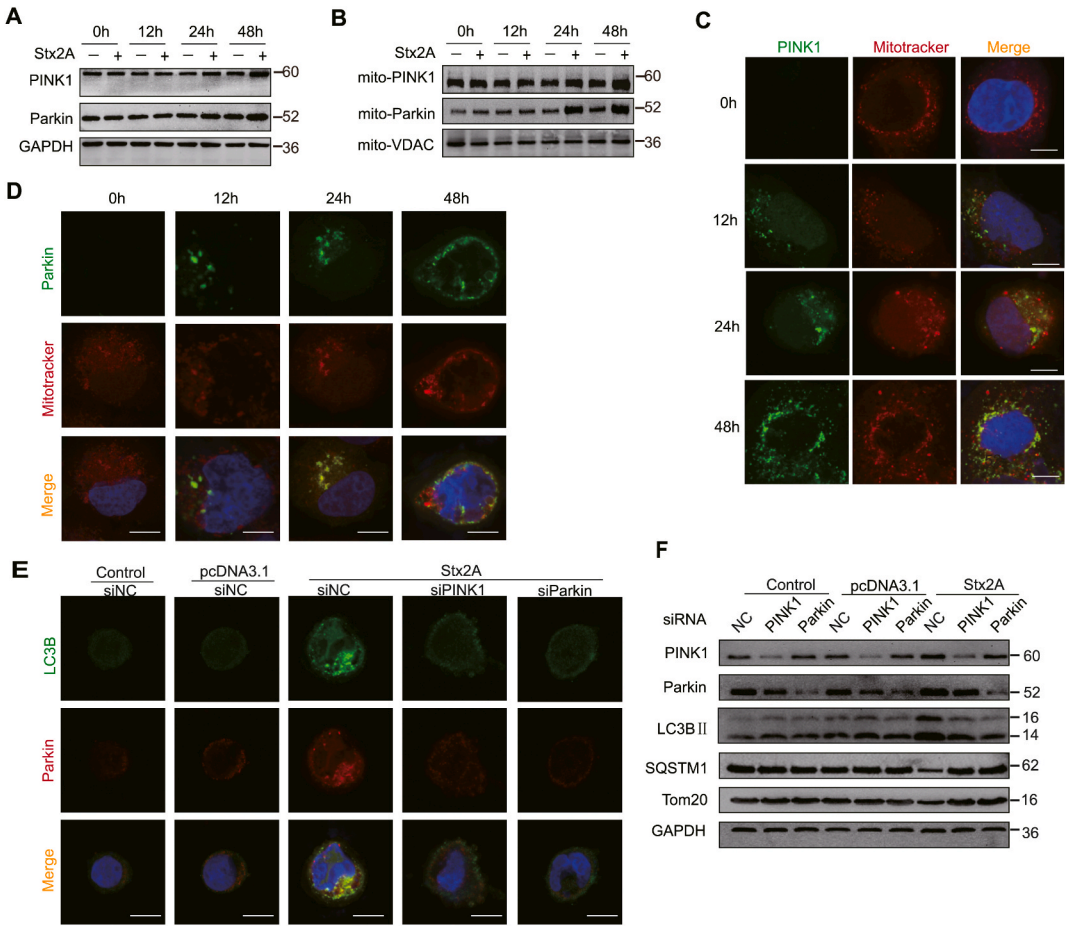

Fig. 3. PINK1 and Parkin mediate Stx2-induced mitophagy in Caco-2 cells. (A–D) Caco-2 cells were transfected with 1 μg/ml Stx2A plasmids for 12, 24 and 48 h. Representative Western blot of PINK1 and Parkin in whole cells (A) as well as PINK1 and Parkin in mitochondria (B), and representative images of PINK1 and MitoTracker immunofluorescence (C) or Parkin and MitoTracker immunofluorescence (D). (E, F) Caco-2 cells were cotransfected with 1 μg/ml Stx2A plasmids and siRNAs, including negative control siRNA (siNC), PINK1 siRNA (siPINK1), or Parkin siRNA (siParkin). Representative images of LC3B (green) and Parkin (red) immunofluorescence (E). Scale bar = 5 μm. The protein expression of PINK1, Parkin, LC3 II/I, Beclin1, Tom20 and SQSTM1 was detected by Western blot analysis (F). n = 3. $^{*}P < 0.05$.

significantly decreased in Caco-2 cells treated with Mito-TEMPO, while SQSTM1 and Tom20 levels were increased in Caco-2 cells treated with Mito-TEMPO (Fig. 4C), indicating that ROS may regulate PINK1/Parkin-dependent mitophagy. To investigate the regulatory role of mitophagy or mitochondrial ROS in apoptosis, Western blot and Annexin V-FITC/PI staining assays were used to detect apoptosis-related proteins or apoptotic cells. After Stx2A transfection, silencing PINK1 or Parkin increased the Bax, Cleaved-Casp3 and Cleaved-Casp9 proapoptotic proteins, and decreased the expression of Bcl-2 (Fig. 4D). In addition, Annexin V–positive Caco-2 cells were increased after Stx2A transfection, and silencing PINK1 or Parkin in addition to Stx2A transfection further increased the number of Annexin V-positive Caco-2 cells (Fig. 4E). Moreover, overactivation of apoptosis by reducing PINK1/Parkin-dependent mitophagy was reversed by Mito-TEMPO (Fig. 4D–E). These results indicated that PINK1/Parkin-dependent mitophagy decreases mitochondrial ROS production and apoptosis induced by Stx2A.

3.5. Stx2A interacts with Tom20

The above results demonstrated that Stx2A induced mitochondrial damage, PINK1/Parkin-dependent mitophagy and apoptosis in intestinal epithelial cells. We next investigated which proteins mediate the mitochondrial damage caused by Stx2A. Flag pull-down and tandem liquid chromatography−mass spectrometry (LC−MS/MS) were used to identify the proteins interacting with Stx2A. Gene Ontology (GO) enrichment analysis indicated that several cellular components were involved in Stx2A-transfected Caco-2 cells, such as intracellular membrane-bound organelles, ribonucleoprotein complexes, ribosomal subunits and mitochondrial protein complexes (Fig. 5A). KEGG pathway enrichment analysis revealed that Stx2A affected multiple signaling pathways, including ribosome biogenesis in eukaryotes, ribosomes, ubiquitin-mediated proteolysis and mitophagy (Fig. 5B). These results indicated that the pathways of the protein synthesis process and mitophagy were affected by Stx2A in Caco-2 cells. Considering that the interaction of

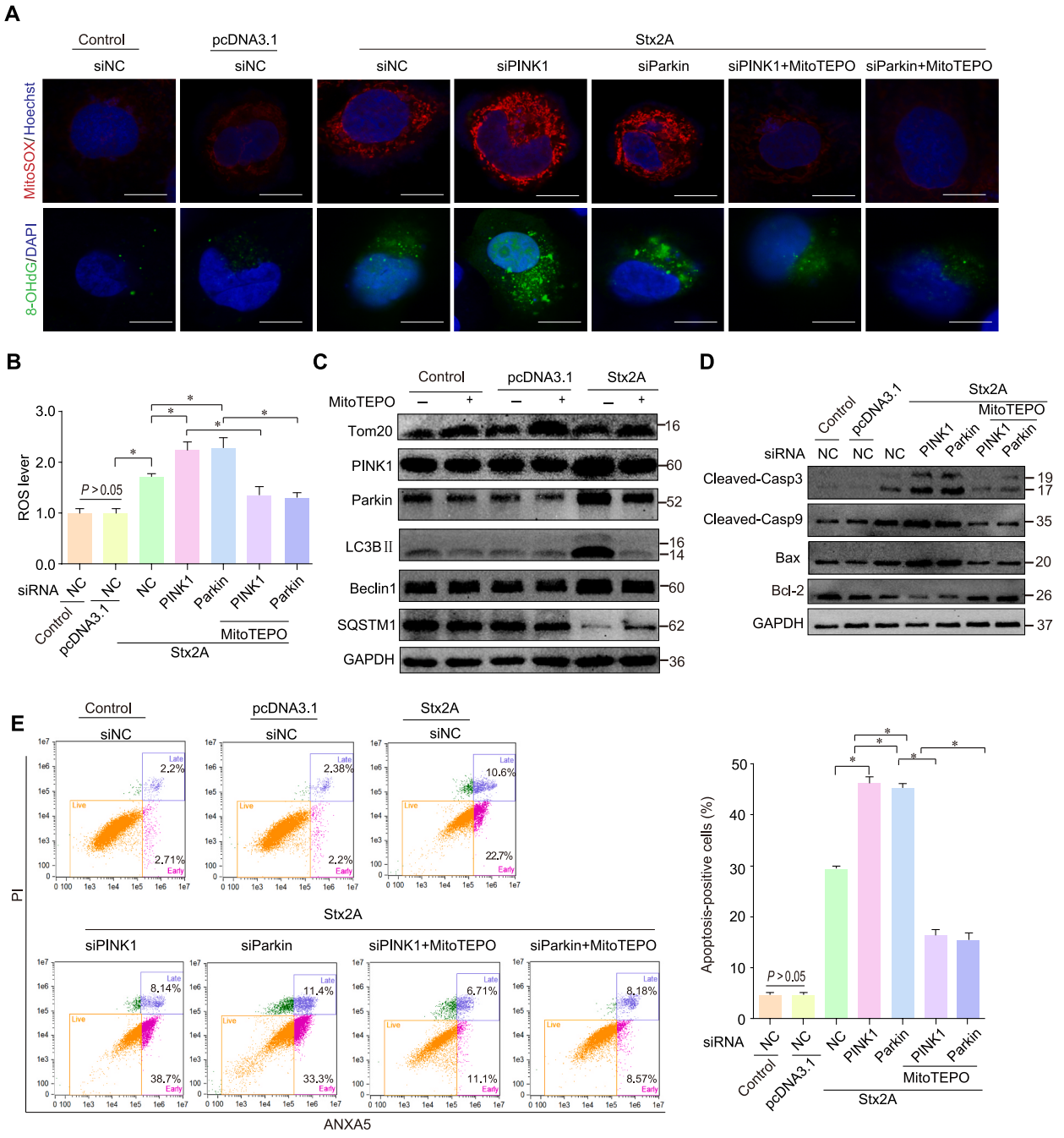

Fig. 4. PINK1/Parkin-dependent mitophagy decreases mitochondrial ROS production and apoptosis induced by Stx2A. (A, B) Caco-2 cells were cotransfected with 1 μg/ml Stx2A plasmids and control siRNA, PINK1 siRNA, or Parkin siRNA. Cells were then treated with MitoTEMPO (100 μM) for 4 h followed by additional culture for 24 h. Representative images of mitochondrial ROS (MitoSOX, Red) and 8-OHdG (Green) immunofluorescence (A) as well as flow cytometry analysis of mitochondrial ROS by MitoSOX (B) in Caco-2 cells. Scale bar = 5 μm. (C) Representative Western blot analysis of PINK1, Parkin, LC3 II/I, Beclin1, Tom20 and SQSTM1 after transfection with 1 μg/ml Stx2A plasmids for 24 h followed by treatment with MitoTEMPO (100 μM) for 4 h. (D, E) Caco-2 cells were treated with or without MitoTEMPO after silencing PINK1 or Parkin and transfection with Stx2A plasmids. Western blot analysis (D) of Cleaved-Caspase-3, Cleaved-Caspase-9, Bax and Bcl-2. Representative images and quantification of cell apoptosis by flow cytometry (E). n = 3. $^*P < 0.05$.

Stx2A with mitochondria requires the binding of mitochondrial outer membrane proteins, we investigated the mitochondrial membrane protein, Tom20. To verify the interaction of Tom20 with Stx2A in vitro, a coimmunoprecipitation (Co-IP) assay was performed using anti-Flag magnetic beads, which demonstrated that significantly more Tom20 was pulled down in the Flag-Stx2A group

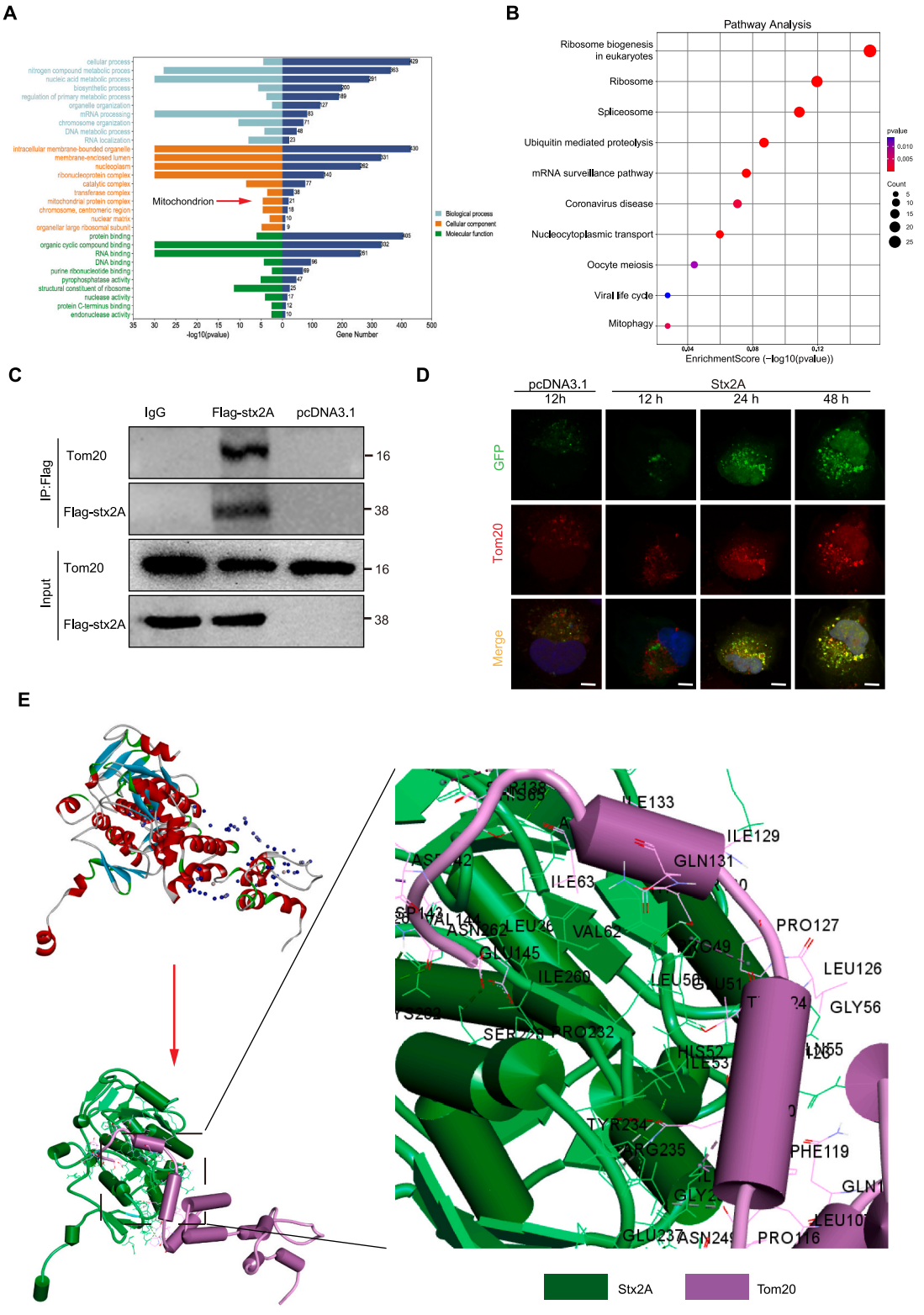

(caption on next page)

Fig. 5. Stx2A interacts with Tom20. (A, B) Protein identification results of LC–MS/MS analysis after transfection with or without Stx2A plasmids were analyzed using DAVID Bioinformatics Resources and visualized using R. Gene Ontology (GO) enrichment analysis (A) is displayed in the form of bar graphs, and the bubble graphs of KEGG pathway analysis (B) show the corresponding enriched pathways. (C) Representative coimmunoprecipitation analysis of the interactions between Tom20 and Stx2A. (D) Colocalization of Stx2A (green) and Tom20 (red). Scale bar = 5 μm. (E) Tom20 (purple) and Stx2A (green) were imported into ZDOCK to simulate possible combinations.

compared to the IgG pull-down control (Fig. 5C). To further determine the interactions between Tom20 and Stx2A, confocal microscopy was employed. Compared to the control cells, Stx2A-transfected cells showed significant colocalization between Tom20 and GFP-Stx2A (Fig. 5D). We utilized ZDOCK to predict potential Tom20-Stx2A contact sites via protein–protein dockings (Fig. 5E), and combine the ZDOCK scores and cluster density to reduce possible atom clashes. Then, we selected the best model with ZDOCK score 17.54 and cluster density 7.0. The results show that residues Gln131, Pro127 and Gly56 of Tom20 are likely involved in the interaction with Stx2A. Overall, these results indicated that Stx2A interacts with Tom20.

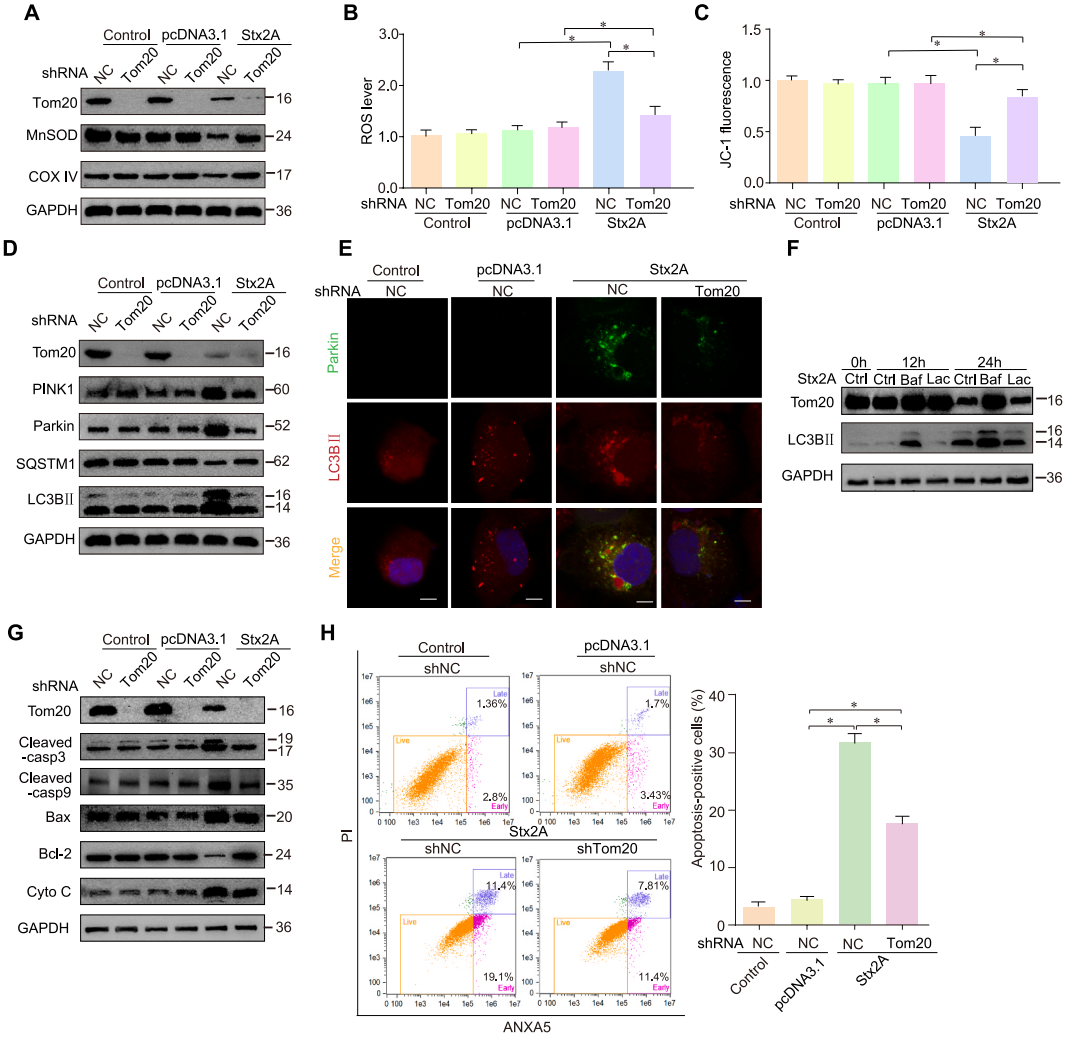

Fig. 6. Stx2A induces mitochondrial damage, mitophagy and apoptosis through Tom20. (A–E) Caco-2 cells were cotransfected with Tom20 shRNA and 1 μg/ml Stx2A plasmids for 24 h. The protein expression levels of MnSOD and COX IV were determined by Western blot analysis (A). Representative images and quantification of mitochondrial superoxide levels (B) and MMP (C) by flow cytometry. Representative Western blot images (D) of PINK1, Parkin, LC3 II/I, Beclin1 and SQSTM1. Representative images of mitophagosomes obtained by LC3B (green) and Parkin (red) (E) immunofluorescence. Scale bar = 5 μm. (F) Caco-2 cells were transfected with Stx2A plasmids for 24 h in the presence or absence of 0.2 μM bafilomycin A1 or 5 μM lactacystin. Representative Western blot of LC3BII and Tom20. (G, H) Caco-2 cells were transfected with Tom20 shRNA and 1 μg/ml Stx2A plasmids for 24 h. Immunoblot analysis (G) of Cleaved-Caspase-3, Cleaved-Caspase-9, Bax, cytochrome *c* (Cyto C) and Bcl-2 in Caco-2 cells. Detection of apoptosis using the annexin V-FITC/PI kit by flow cytometry (H). n = 3. $^*P < 0.05$.

3.6. Stx2A induces mitochondrial damage, mitophagy and apoptosis through Tom20

We further investigated whether Stx2A induces mitochondrial damage, mitophagy and apoptosis through Tom20. Knockdown of Tom20 significantly attenuated the decrease in MnSOD, COXIV and mitochondrial membrane potential as well as the increase in ROS accumulation (Fig. 6A–C). In addition, knockdown of Tom20 significantly restored the increase in Pink1, Parkin and LC3BII as well as the decrease in SQSTM1 in Stx2A-transfeected cells (Fig. 6D). Compared to control cells, Stx2A-transfected cells showed significant colocalization between LC3BII and Parkin, but little colocalization was observed in Tom20 knockdown cells, which indicated that knockdown of Tom20 significantly inhibited Parkin-mediated mitophagy induced by Stx2A (Fig. 6E). Previous results have indicated that the expression of Tom20 protein decreases after Stx2A stimulation. To determine whether the degradation of Tom20 is a function

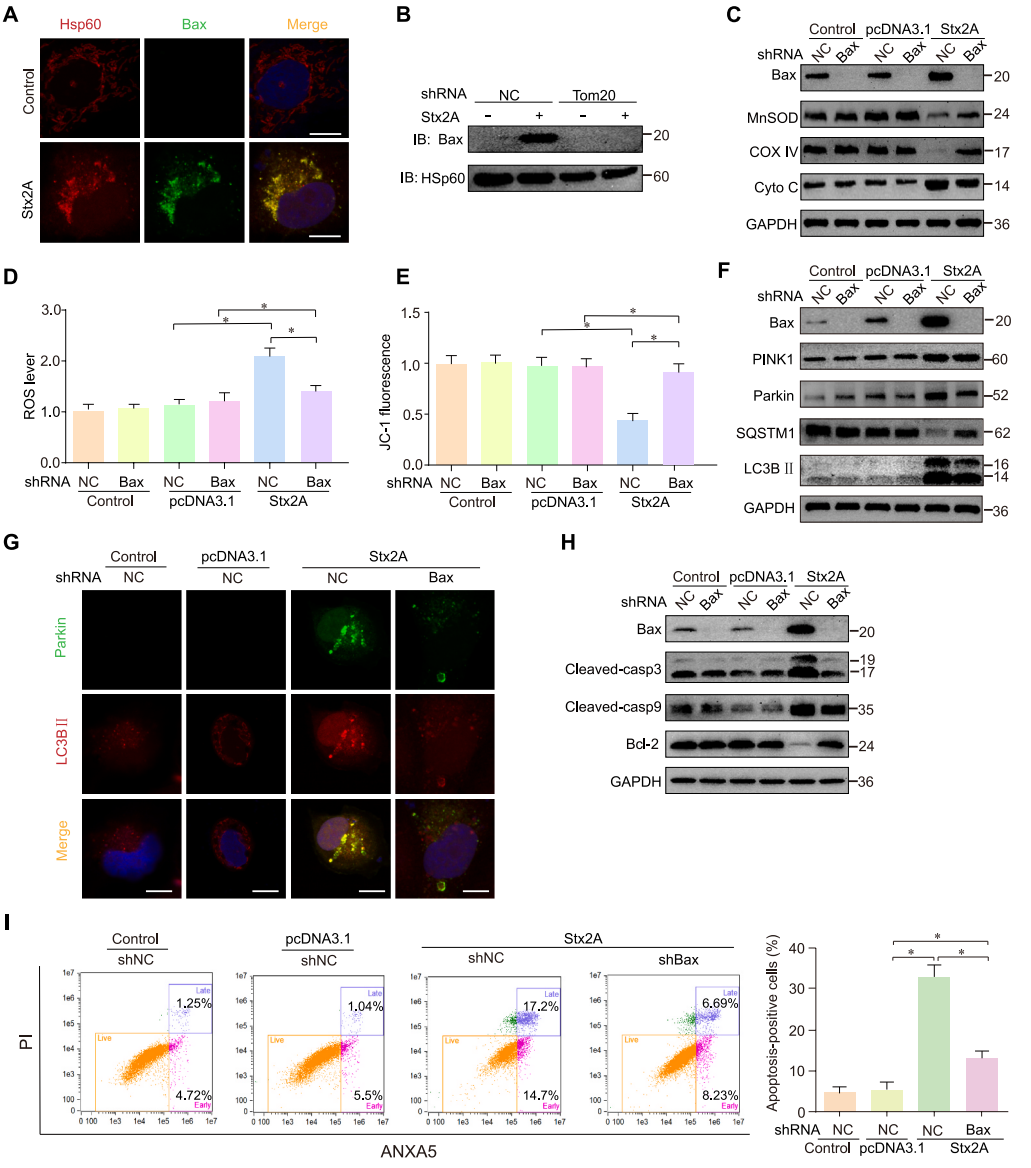

Fig. 7. Tom20-induced translocation of Bax to mitochondria contributes to mitochondrial damage, mitophagy and apoptosis. (A) Bax (green) translocated to mitochondria after transfection with 1 μg/ml Stx2A plasmids. Hsp60 (red) was localized to mitochondria. Scale bar = 5 μm. (B) Knockdown of Tom20 blocked the translocation of Bax to mitochondria after Stx2A transfection. (C–I) Caco-2 cells were transfected with Bax shRNA and Stx2A plasmids for 24 h. The protein expression levels of MnSOD and COX IV were determined by Western blot analysis (C). Representative images of mitochondrial superoxide levels (D) and MMP (E) by flow cytometry. Representative Western blot images (F) of PINK1, Parkin, LC3 II/I, Beclin1 and SQSTM1. Representative immunofluorescence images of mitophagosomes (G) with LC3B and Parkin. Western blot analysis (H) of Cleaved-Caspase-3, Cleaved-Caspase-9, Bax, cytochrome *c* (Cyto C) and Bcl-2 in Caco-2 cells. Apoptosis was detected using an annexin V-FITC/PI kit and flow cytometry (I). n = 3. *$P < 0.05$.

of protease or mitophagy, Western blot assay was used to detect the expression of Tom20 in Caco-2 cells treated with the proteasome inhibitor, lactacystin, and the mitophagy inhibitor, bafilomycin A1. As shown in Fig. 6F, bafilomycin A1, but not lactacystin, significantly restored Tom20 expression, which indicated that the degradation of Tom20 by Stx2A was required for mitophagy. We next investigated whether Tom20 is involved in Stx2A-induced apoptosis. Knockdown of Tom20 significantly decreased the expression of Cleaved-Caspase-3, Bax, Cleaved-Caspase-9 and Cyto C, and increased Bcl-2 expression in Caco-2 cells after Stx2A transfection (Fig. 6G). Flow cytometry also showed that knockdown of Tom20 reduced Annexin V–positive cells in Stx2A-transfected Caco-2 cells (Fig. 6H). Collectively, these results indicated that Stx2A induces mitochondrial damage, mitophagy and apoptosis through Tom20.

3.7. *Tom20-induced translocation of bax to mitochondria contributes to mitochondrial damage, mitophagy and apoptosis*

A previous study has reported that the Tom complex is important for Bax mitochondrial localization to induce mitochondrial damage [24]. Thus, we investigated whether Tom20 is involved in Stx2A-induced mitochondrial damage, mitophagy and apoptosis via Bax regulation. As shown in Fig. 7A–B, Stx2A significantly induced Bax translocation from the cytoplasm to mitochondria, while the effect of Bax translocation to mitochondria was abolished by Tom20 knockdown, which indicated that Stx2A induced Tom20-dependent mitochondrial localization of Bax. Moreover, knockdown of Bax not only alleviated the increase in Stx2A-induced cytochrome *c* (Fig. 7C) but also suppressed mitochondrial damage, including restoring the reduction in MnSOD and COXIV (Fig. 7C) as

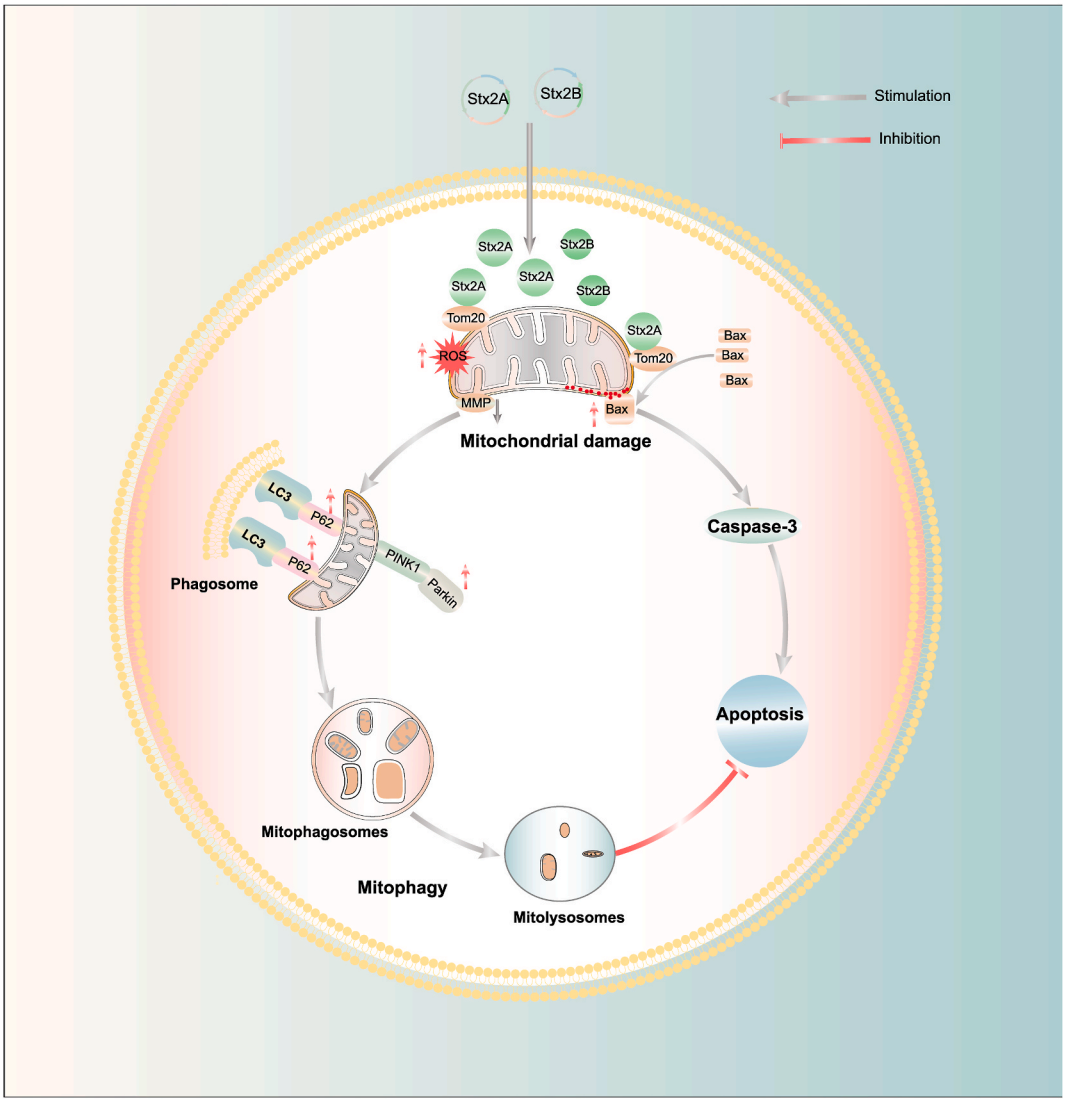

Fig. 8. Schematic representation of mitochondrial damage, mitophagy and apoptosis in Caco-2 cells. Stx2A causes the mitochondrial damage of Caco-2 cells, which induces mitophagy and apoptosis activation via the interaction of Tom20 in Caco-2 cells, and PINK1/Parkin–mediated mitophagy ameliorates apoptosis by eliminating damaged mitochondria.

well as reducing the production of mitochondrial ROS (Fig. 7D) and restoring the reduced mitochondrial membrane potential (Fig. 7E). Moreover, knockdown of Bax decreased the protein expression of Parkin and LC3BII but increased the expression of SQSTM1 in Stx2A-transfected Caco-2 cells (Fig. 7F). Immunofluorescence assays also showed that the colocalization of LC3BII and Parkin was significantly weakened in Stx2A-transfected Caco-2 cells after silencing Bax, which indicated that Bax knockdown inhibited Stx2A-induced mitophagy (Fig. 7G). In addition, knockdown of Bax significantly decreased apoptotic proteins, including Cleaved-Caspase-3 and Cleaved-Caspase-9, but increased Bcl-2 expression (Fig. 7H). Flow cytometry also showed that knockdown of Bax restored Stx2A-induced apoptosis (Fig. 7I). Altogether, these results indicated that Stx2A binding to Tom20 recruits Bax to mitochondria, which promotes mitochondrial damage, mitophagy and apoptosis in Caco-2 cells.

4. Discussion

Shiga toxin 2 induces apoptosis of intestinal epithelial cells and plays a role in hemorrhagic colitis. However, the crosstalk between Stx2A and the induction of apoptosis is not completely understood. In the present study, we demonstrated that Stx2A induces mitochondrial damage, mitophagy and apoptosis via the interaction of Tom20 in Caco-2 cells, and Stx2A-induced mitophagy ameliorates apoptosis by eliminating damaged mitochondria. This new mechanism by which Stx2A leads to apoptosis involves the following process: (i) Stx2A induces mitochondrial damage, PINK1/Parkin-dependent mitophagy and apoptosis; (ii) PINK1/Parkin-dependent mitophagy decreases mitochondrial ROS production and apoptosis induced by Stx2A; (iii) Stx2A interacts with TOM20; and (iv) Tom20-induced translocation of Bax to mitochondria contributes to mitochondrial damage, mitophagy and apoptosis. These findings help to explain the deleterious effects of Stx2A on mitochondria and intestinal epithelial cells through the interaction of Tom20 (Fig. 8).

Shiga toxins have been reported to induce apoptosis of intestinal epithelial cells by the mitochondria-dependent pathway, ribotoxic stress, autophagy, the endoplasmic reticulum stress pathway and other pathways [21,25,26]. However, the underlying molecular mechanism of apoptosis induced by Stxs remains unclear in intestinal epithelial cells. A previous study has reported that Stx1-induced apoptosis is accompanied by mitochondrial membrane damage in HeLa cells [14]. Thus, we speculated that the apoptosis of HeLa cells induced by Stx1 may be caused by mitochondrial damage. In the present study, we found that Stx2A activated mitochondrial ROS production and decreased mitochondrial membrane potential in Caco-2 cells. In addition, Stx2A markedly decreased the expression of MnSOD and COX IV protein levels as well as increased structural damage to mitochondria. By reducing mitochondrial ROS release, MitoTEMPO lowered the activation of apoptosis. These results indicated that Stx2A-induced mitochondrial damage is the trigger of apoptosis in Caco-2 cells.

However, the mechanism underlying the Stx2A-activated mitochondrial apoptotic pathway remains unclear. Mitochondria are important organelles that have multiple functions in cell metabolism and homeostasis [27,28]. Approximately 99% of mitochondrial proteins are made in the cytosol as precursors, and they are then transported into mitochondria by translocase outer membrane (TOM) complexes and the translocase inner membrane (TIM) [29]. The most significant channel-forming protein in the TOM complex, Tom20, is responsible for identifying mitochondrial-target signals in the proteins and connecting the sequence to the Tom40 complex [30]. In the present study, we demonstrated that Stx2A induced mitochondrial damage, mitophagy and apoptosis through the interaction of Tom20. In addition, after Tom20 recruited Bax to the outer mitochondrial membrane, Bax promoted the aggregation of mitochondria, which promoted the release of cytochrome *c* and ROS into the cytosol, thereby initiating the apoptosis signal of Caco-2 cells. Therefore, mitochondria may act as an organelle connecting Stx2A-induced apoptosis via Tom20 molecules.

Mitophagy and mitochondrial biogenesis are two dynamically balanced and tightly regulated processes that are essential for preserving mitochondrial homeostasis and cellular adaptability in response to stress [31]. Mitophagy is a process in which cells selectively remove damaged mitochondria, and the formation of mitophagosomes is the gold standard of mitophagy [32]. In the present study, the TEM results indicated that Stx2A led to ultrastructural lesions of Caco-2 cells with typical mitophagosomes. In addition, Stx2A increased the expression levels of LC3BII and Beclin1 but decreased the expression levels of SQSTM1 and Tom20 in a time-dependent manner. Immunofluorescence staining of LC3B and MitoTracker also demonstrated that Stx2A induced mitophagy in Caco-2 cells. Furthermore, PINK1 and Parkin mediated Stx2A-induced mitophagy, while knockdown of PINK1 or Parkin decreased Stx2A-induced Parkin-mediated mitophagy. Taken together, these results suggested that Stx2A triggers PINK1/Parkin-mediated mitophagy in Caco-2 cells.

Accumulating evidence suggests that PINK1/Parkin-mediated mitophagy protects against apoptosis caused by antitumor drugs, toxins and other substances [19,33,34]. In healthy mitochondria, PINK1 is naturally incorporated into the inner membrane and quickly destroyed through proteolytic degradation to maintain low expression [35]. Upon mitochondrial damage, such as depolarization, PINK1 accumulates on the outer mitochondrial membrane and promotes the phosphorylation of Parkin, which ubiquitinates mitochondrial outer membrane proteins and delivers ubiquitin mitochondria to autophagosomes by binding to SQSTM1 and LC3B, thereby activating mitophagy and eliminating damaged mitochondria [36]. In the present study, we demonstrated that PINK1/Parkin-dependent mitophagy protected against Stx2A-induced apoptosis in Caco-2 cells. When exposed to Stx2A, a deficiency of PINK1 or Parkin increased mitochondrial ROS production and apoptosis activation, while overactivation of apoptosis due to inhibition of mitophagy was reversed by MitoTEMPO. Thus, these findings suggested that mitochondrial clearance by mitophagy attenuates Stx2A-induced apoptosis.

However, the study had limitations. Based on the findings of this study, we propose that Stx2A induces mitochondrial damage, mitophagy and apoptosis through its interaction with Tom20, while mitophagy caused by Stx2A improves apoptosis by eliminating damaged mitochondria in Caco-2 cells. Further extensive investigation is needed to confirm the findings, especially lack of animal testing. Further studies in cells and animals infected with Stx2A knockout strains will be conducted to confirm the pathogenic role of

Stx2A. In addition, we need to further validate that the Tom20 interaction dependent apoptosis induced by the Stx2A protein is entirely dependent/independent of this interaction. Based on the binding sites between Stx2A and Tom20, we will construct relevant mutants to confirm the role of this interaction in apoptosis.

In conclusion, we determined that Stx2A induces mitochondrial damage, PINK1/Parkin-mediated mitophagy and apoptosis via the interaction of Tom20 in Caco-2 cells, and we also demonstrated that mitophagy ameliorates apoptosis by eliminating damaged mitochondria. These findings provide a better understanding of how Stx2A induces mitophagy and injures intestinal epithelial cells.

Data availability statement

Data associated with this study has been deposited at The data of the LC−MS/MS analysis has been deposited to the ProteomeXchange Consortium (http://proteomecentral.proteomexchange.org) via the iProX partner repository with the dataset identifier PXD038256.

Author contribution statement

Jie Tang; Xiaoxue Lu: Conceived and designed the experiments; Performed the experiments; Analyzed and interpreted the data; Wrote the paper. Tao Zhang; Yuyang Feng; Qiaolin Xu; Jing Li; Yuanzhi Lan and Huaxing Luo: Contributed reagents, materials, analysis tools or data. Linghai Zeng; Yuanyuan Xiang; Yan Zhang; Qian Li and Xuhu Mao: Analyzed and interpreted the data. Bin Tang; Dongzhu Zeng: Conceived and designed the experiments; Contributed reagents, materials, analysis tools or data; Analyzed and interpreted the data; Wrote the paper.

Declaration of competing interest

The authors declare that they have no known competing financial interests or personal relationships that could have appeared to influence the work reported in this paper.

Acknowledgements

This work was supported by grants from the Natural Science Foundation of Chongqing (no. cstc2020jcyjmsxmX0220) and the Scientific Research Incubation Project, The Third Affiliated Hospital of Chongqing Medical University (no. KY20079).

Appendix A. Supplementary data

Supplementary data to this article can be found online at https://doi.org/10.1016/j.heliyon.2023.e20012.

References

[1] A. Melton-Celsa, K. Mohawk, L. Teel, A. O'Brien, Pathogenesis of Shiga-toxin producing escherichia coli, Curr. Top. Microbiol. Immunol. 357 (2012) 67–103.
[2] A.D. O'Brien, R.K. Holmes, Shiga and shiga-like toxins, Microbiol. Rev. 51 (2) (1987) 206–220.
[3] Y. Endo, K. Tsurugi, T. Yutsudo, Y. Takeda, T. Ogasawara, K. Igarashi, Site of action of a Vero toxin (VT2) from Escherichia coli O157:H7 and of Shiga toxin on eukaryotic ribosomes. RNA N-glycosidase activity of the toxins, Eur. J. Biochem. 171 (1–2) (1988) 45–50.
[4] T.G. Obrig, T.P. Moran, J.E. Brown, The mode of action of Shiga toxin on peptide elongation of eukaryotic protein synthesis, Biochem. J. 244 (2) (1987) 287–294.
[5] C.A. Lingwood, Role of verotoxin receptors in pathogenesis, Trends Microbiol. 4 (4) (1996) 147–153.
[6] C.A. Lingwood, H. Law, S. Richardson, M. Petric, J.L. Brunton, S. De Grandis, M. Karmali, Glycolipid binding of purified and recombinant Escherichia coli produced verotoxin in vitro, J. Biol. Chem. 262 (18) (1987) 8834–8839.
[7] V.L. Tesh, Activation of cell stress response pathways by Shiga toxins, Cell Microbiol. 14 (1) (2012) 1–9.
[8] M.S. Lee, S. Koo, D.G. Jeong, V.L. Tesh, Shiga toxins as multi-functional proteins: induction of host cellular stress responses, role in pathogenesis and therapeutic applications, Toxins 8 (3) (2016).
[9] E. Rath, A. Moschetta, D. Haller, Mitochondrial function - gatekeeper of intestinal epithelial cell homeostasis, Nat. Rev. Gastroenterol. Hepatol. 15 (8) (2018) 497–516.
[10] J. Dan Dunn, L.A. Alvarez, X. Zhang, T. Soldati, Reactive oxygen species and mitochondria: a nexus of cellular homeostasis, Redox Biol. 6 (2015) 472–485.
[11] V.L. Tesh, Induction of apoptosis by Shiga toxins, Future Microbiol. 5 (3) (2010) 431–453.
[12] J. Davidson, A. Kerr, K. Guy, D. Rotondo, Prostaglandin and fatty acid modulation of Escherichia coli O157 phagocytosis by human monocytic cells, Immunology 94 (2) (1998) 228–234.
[13] A. Pinto, C. Berdasco, D. Arenas-Mosquera, A. Cangelosi, P.A. Geoghegan, M.C. Nuñez, J. Goldstein, Anti-inflammatory agents reduce microglial response, demyelinating process and neuronal toxin uptake in a model of encephalopathy produced by Shiga Toxin 2, Int. J. Med. Microbiol. 308 (8) (2018) 1036–1042.
[14] J. Fujii, T. Matsui, D.P. Heatherly, K.H. Schlegel, P.I. Lobo, T. Yutsudo, G.M. Ciraolo, R.E. Morris, T. Obrig, Rapid apoptosis induced by Shiga toxin in HeLa cells, Infect. Immun. 71 (5) (2003) 2724–2735.
[15] G. Ashrafi, T.L. Schwarz, The pathways of mitophagy for quality control and clearance of mitochondria, Cell Death Differ. 20 (1) (2013) 31–42.
[16] P. Sulkshane, J. Ram, A. Thakur, N. Reis, O. Kleifeld, M.H. Glickman, Ubiquitination and receptor-mediated mitophagy converge to eliminate oxidation-damaged mitochondria during hypoxia, Redox Biol. 45 (2021), 102047.
[17] M.S. Lee, R.P. Cherla, M.H. Jenson, D. Leyva-Illades, M. Martinez-Moczygemba, V.L. Tesh, Shiga toxins induce autophagy leading to differential signalling pathways in toxin-sensitive and toxin-resistant human cells, Cell Microbiol. 13 (10) (2011) 1479–1496.

[18] B. Tang, Q. Li, X.H. Zhao, H.G. Wang, N. Li, Y. Fang, K. Wang, Y.P. Jia, P. Zhu, J. Gu, J.X. Li, Y.J. Jiao, W.D. Tong, M. Wang, Q.M. Zou, F.C. Zhu, X.H. Mao, Shiga toxins induce autophagic cell death in intestinal epithelial cells via the endoplasmic reticulum stress pathway, Autophagy 11 (2) (2015) 344–354.
[19] Q. Lin, S. Li, N. Jiang, X. Shao, M. Zhang, H. Jin, Z. Zhang, J. Shen, Y. Zhou, W. Zhou, L. Gu, R. Lu, Z. Ni, PINK1-parkin pathway of mitophagy protects against contrast-induced acute kidney injury via decreasing mitochondrial ROS and NLRP3 inflammasome activation, Redox Biol. 26 (2019), 101254.
[20] B. Zhou, J.Y. Zhang, X.S. Liu, H.Z. Chen, Y.L. Ai, K. Cheng, R.Y. Sun, D. Zhou, J. Han, Q. Wu, Tom20 senses iron-activated ROS signaling to promote melanoma cell pyroptosis, Cell Res. 28 (12) (2018) 1171–1185.
[21] J.Y. Park, Y.J. Jeong, S.K. Park, S.J. Yoon, S. Choi, D.G. Jeong, S.W. Chung, B.J. Lee, J.H. Kim, V.L. Tesh, M.S. Lee, Y.J. Park, Shiga toxins induce apoptosis and ER stress in human retinal pigment epithelial cells, Toxins 9 (10) (2017).
[22] D.J. Klionsky, A.K. Abdel-Aziz, S. Abdelfatah, M. Abdellatif, A. Abdoli, S. Abel, H. Abeliovich, M.H. Abildgaard, Y.P. Abudu, A. Acevedo-Arozena, I. E. Adamopoulos, K. Adeli, T.E. Adolph, A. Adornetto, E. Aflaki, G. Agam, A. Agarwal, B.B. Aggarwal, M. Agnello, P. Agostinis, J.N. Agrewala, A. Agrotis, P. V. Aguilar, S.T. Ahmad, Z.M. Ahmed, U. Ahumada-Castro, S. Aits, S. Aizawa, Y. Akkoc, T. Akoumianaki, H.A. Akpinar, A.M. Al-Abd, L. Al-Akra, A. Al-Gharaibeh, M.A. Alaoui-Jamali, S. Alberti, E. Alcocer-Gómez, C. Alessandri, M. Ali, M.A. Alim Al-Bari, S. Aliwaini, J. Alizadeh, E. Almacellas, A. Almasan, A. Alonso, G. D. Alonso, N. Altan-Bonnet, D.C. Altieri, É.M.C. Á, S. Alves, C. Alves da Costa, M.M. Alzaharna, M. Amadio, C. Amantini, C. Amaral, S. Ambrosio, A.O. Amer, V. Ammanathan, Z. An, S.U. Andersen, S.A. Andrabi, M. Andrade-Silva, A.M. Andres, S. Angelini, D. Ann, U.C. Anozie, M.Y. Ansari, P. Antas, A. Antebi, Z. Antón, T. Anwar, L. Apetoh, N. Apostolova, T. Araki, Y. Araki, K. Arasaki, W.L. Araújo, J. Araya, C. Arden, M.A. Arévalo, S. Arguelles, E. Arias, J. Arikkath, H. Arimoto, A.R. Ariosa, D. Armstrong-James, L. Arnauné-Pelloquin, A. Aroca, D.S. Arroyo, I. Arsov, R. Artero, D. Asaro, M. Aschner, Ashrafizadeh, Guidelines for the use and interpretation of assays for monitoring autophagy, in: 1), Autophagy, fourth ed., 2021, pp. 1–382, 17 (1).
[23] E.P. Bulthuis, M. Adjobo-Hermans, P. Willems, W. Koopman, Mitochondrial morphofunction in mammalian cells, antioxid, Redox Signal 30 (18) (2019) 2066–2109.
[24] T.T. Renault, O. Teijido, B. Antonsson, L.M. Dejean, S. Manon, Regulation of Bax mitochondrial localization by Bcl-2 and Bcl-x(L): keep your friends close but your enemies closer, Int. J. Biochem. Cell Biol. 45 (1) (2013) 64–67.
[25] N.L. Jones, A. Islur, R. Haq, M. Mascarenhas, M.A. Karmali, M.H. Perdue, B.W. Zanke, P.M. Sherman, Escherichia coli Shiga toxins induce apoptosis in epithelial cells that is regulated by the Bcl-2 family, Am. J. Physiol. Gastrointest. Liver Physiol. 278 (5) (2000) G811–G819.
[26] M.S. Lee, H. Kwon, E.Y. Lee, D.J. Kim, J.H. Park, V.L. Tesh, T.K. Oh, M.H. Kim, Shiga toxins activate the NLRP3 inflammasome pathway to promote both production of the proinflammatory cytokine interleukin-1β and apoptotic cell death, Infect. Immun. 84 (1) (2016) 172–186.
[27] S.A. Killackey, D.J. Philpott, S.E. Girardin, Mitophagy pathways in health and disease, J. Cell Biol. 219 (11) (2020).
[28] Z. Cheng, M. Ristow, Mitochondria and metabolic homeostasis, Antioxidants Redox Signal. 19 (3) (2013) 240–242.
[29] O. Schmidt, N. Pfanner, C. Meisinger, Mitochondrial protein import: from proteomics to functional mechanisms, Nat. Rev. Mol. Cell Biol. 11 (2010) 655–667.
[30] J. Su, D. Liu, F. Yang, M.Q. Zuo, C. Li, M.Q. Dong, et al., Structural basis of Tom20 and Tom22 cytosolic domains as the human TOM complex receptors, Proc. Natl. Acad. Sci. U.S.A. 119 (2022), e2200158119.
[31] J. Zhu, K.Z. Wang, C.T. Chu, After the banquet: mitochondrial biogenesis, mitophagy, and cell survival, Autophagy 9 (2013) 1663–1676.
[32] T.N. Nguyen, B.S. Padman, M. Lazarou, Deciphering the molecular signals of PINK1/parkin mitophagy, Trends Cell Biol. 26 (2016) 733–744.
[33] X. Gu, Y. Qi, Z. Feng, L. Ma, K. Gao, Y. Zhang, Lead (Pb) induced ATM-dependent mitophagy via PINK1/Parkin pathway, Toxicol. Lett. 291 (2018) 92–100.
[34] Y.Y. Xiao, J.X. Xiao, X.Y. Wang, T. Wang, X.H. Qu, L.P. Jiang, et al., Metformin-induced AMPK activation promotes cisplatin resistance through PINK1/Parkin dependent mitophagy in gastric cancer, Front. Oncol. 12 (2022), 956190.
[35] D.P. Narendra, S.M. Jin, A. Tanaka, D.F. Suen, C.A. Gautier, J. Shen, et al., PINK1 is selectively stabilized on impaired mitochondria to activate Parkin, PLoS Biol. 8 (2010), e1000298.
[36] J.W. Harper, A. Ordureau, J.M. Heo, Building and decoding ubiquitin chains for mitophagy, Nat. Rev. Mol. Cell Biol. 19 (2018) 93–108.